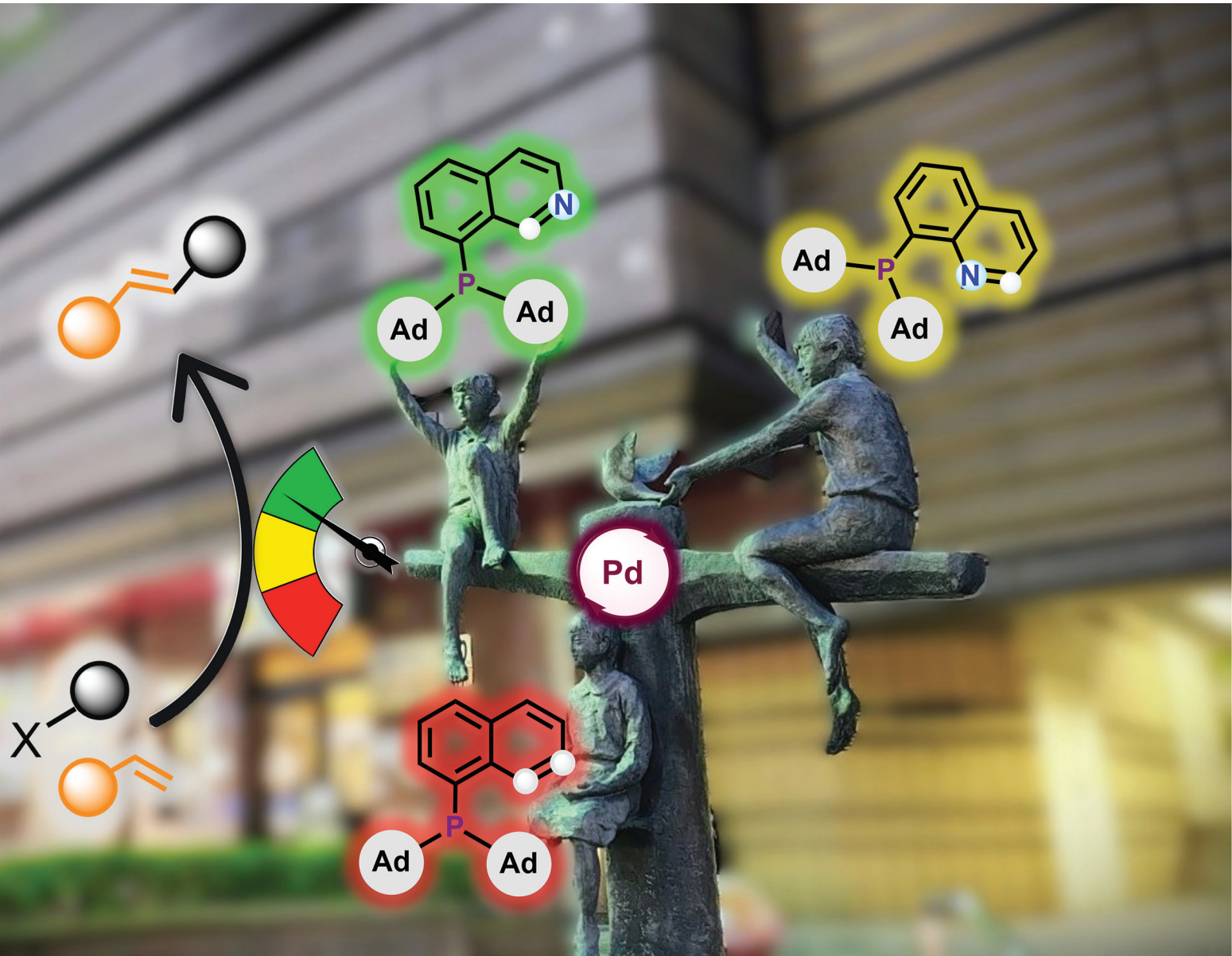


Dalton Transactions

An international journal of inorganic chemistry

rsc.li/dalton



ISSN 1477-9226

COMMUNICATION

[View Article Online](#)
[View Journal](#) | [View Issue](#)


Cite this: *Dalton Trans.*, 2025, **54**, 17073

Received 21st October 2025,
Accepted 29th October 2025

DOI: 10.1039/d5dt02523k

rsc.li/dalton

P(1-Ad)₂ (Ad = adamantyl) moiety-substituted quinoline, naphthyl, and isoquinoline ligands were synthesized to make Pd(II) complexes with $\kappa^2\text{-P}^{\text{N}}/\text{P}^{\text{C}}$ coordination. Pd-based catalytic activity towards Mizoroki–Heck coupling of those phosphine ligands was examined, showing that the ligand *i*QAdPhos (L3) with an isoquinoline core possessing $\kappa^2\text{-P}^{\text{C}}$ coordination was superior.

Ligand design and understanding its pivotal role in catalytic reactions is a fascinating field of organometallic chemistry, which keeps evolving.^{1–3} The electronic nature and bulkiness of the substituent on the ligating site play a key role in tuning the catalytic activity, particularly for phosphine ligands.^{4–7} Over time, the P^P ligand core^{8–11} evolved into P^N or P^C type coordinating ligands, wherein N or C acts as a σ-donor.^{12–29} The DalPhos class of ligands [P(1-Ad)₂(Ar); Ar = *o*-C₆H₄-NR₂] with phosphorus bearing bulky adamantyl (Ad) and P^N type coordination is crucial for C–N coupling using NH₃ (Fig. 1A).^{28,29} Using the DalPhos ligand, catalytic systems with Pd²⁹ and Ni³⁰ were extensively studied by Stradiotto and coworkers. At the same time, (DalPhos)-Au complexes are being explored by Patil and coworkers in various alkene difunctionalization reactions,³¹ suggesting the importance of P^N coordination where the N atom is sp³ in nature. Interestingly, P^N coordination with an sp²-type nitrogen is not extensively used for catalysis.^{26,32,33} The quinoline core having PPh₂ or P(*i*Pr)₂ at the 8th position resulted in $\kappa^2\text{-P}^{\text{N}}$ coordinated metal complexes and their properties were studied (Fig. 1B).^{12,34–37}

Metalation or deprotonation of a C–H bond in proximity to the phosphorus center led to the formation of P^C-coordinated Pd(II) complexes (Fig. 1C).^{38–42} The $\kappa^2\text{-P}^{\text{C}}$ ligated [P(Ph₂)(1-naphthyl)Pd(OAc)]₂ exhibited catalytic activity for the Mizoroki–Heck reaction,^{43,44} affording 55% C–C coupled product (1 mol% catalyst; 130 °C; TOF = 61 h^{–1}).³⁸ For the isoquinoline core with PPh₂ substitution at the 8th position, the

[Di(1-adamantyl)][aryl]phosphine ligands: synthesis, palladium complexation, and catalytic activity

Chinraj Sivarajan and Raja Mitra *

$\kappa^2\text{-P}^{\text{C}}$ ligated Ru complex was synthesized, and its reactivity was studied (Fig. 1D);⁴⁵ however, the catalytic activity was not investigated. We envisage that changing the aromatic ring attached to the di(1-adamantyl)phosphine {P(1-Ad)₂} moiety might lead to controllable $\kappa^2\text{-P}^{\text{N}}/\text{P}^{\text{C}}$ coordination towards Pd. Herein, we report P(1-Ad)₂ on quinoline, naphthyl, and isoquinoline cores as ligands, their coordination chemistry towards Pd, and their catalytic applications (Fig. 1E).

Following the literature,^{46,47} di(1-adamantyl)phosphinic acid chloride was synthesized from adamantane using AlCl₃ and PCl₃, and it was further reduced using LiAlH₄ to obtain air-sensitive di(1-adamantyl)phosphine {(1-Ad)₂PH} (Fig. 2A).⁴⁷ The synthesized (1-Ad)₂PH was immediately used in Pd-catalyzed C–P coupling⁴⁷ with the corresponding aryl bromide to give the desired ligands (L1–3). 8-Bromoquinoline was used to synthesize 8-(di(1-adamantyl)phosphino)quinoline (QAdPhos; L1). 1-(Di(1-adamantyl)phosphino)naphthalene (NAdPhos; L2) was derived from 1-bromonaphthalene, and 8-(di(1-adaman-

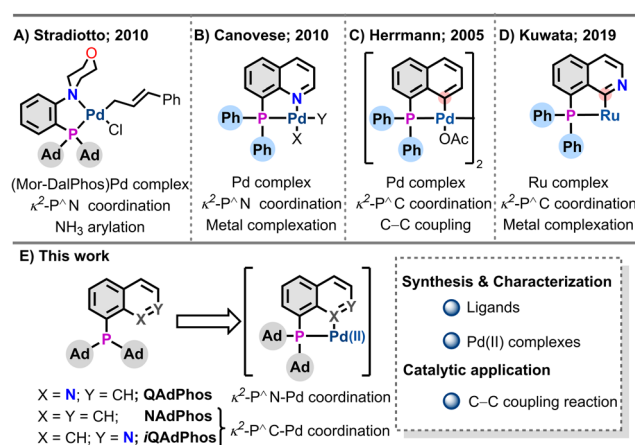


Fig. 1 (A) (Mor-DalPhos)Pd precatalyst. (B), (C) and (D) Previously reported PPh₂ analogue with an aromatic core showing a P^N/P^C coordination bound metal centre. (E) This work: P(1-Ad)₂ substituted ligand with an aromatic core and corresponding Pd complexes.



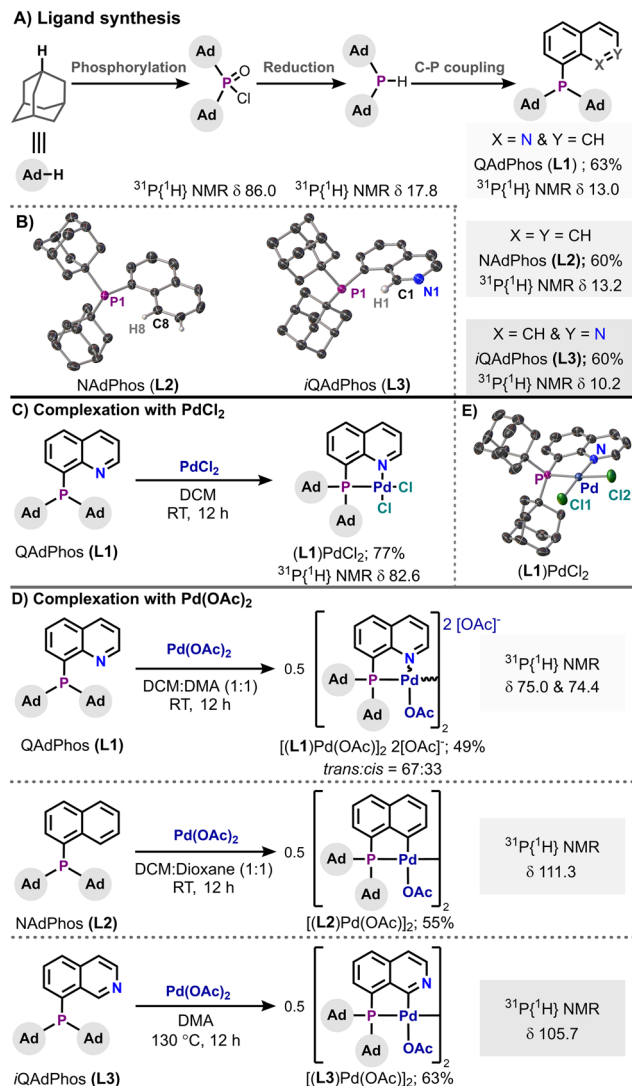


Fig. 2 (A) Synthesis of ligands (**L1–3**); ${}^{31}\text{P}\{\text{H}\}$ NMR spectra recorded in CDCl_3 ; δ in ppm. (B) Crystal structures of **L2** and **L3** (shown at a 50% probability of thermal ellipsoids; most of the H atoms are omitted for clarity). (C) and (D) Synthesis of $\text{Pd}(\text{II})$ complexes with **L1**, **L2**, and **L3**. (E) Crystal structure of the $(\text{L1})\text{PdCl}_2\cdot 3\text{CH}_2\text{Cl}_2$ complex (shown at a 50% probability of thermal ellipsoids; DCM solvents and H atoms are omitted for clarity). See the SI for details.

tyl)phosphino)isoquinoline (*i*QAdPhos; **L3**) was derived from 8-bromoisoquinoline (Fig. 2A).

${}^{31}\text{P}\{\text{H}\}$ NMR showed a single peak of **L1** at 13.0 ppm, that of **L2** at 13.2 ppm, and that of **L3** at 10.2 ppm in CDCl_3 . The P atom in these ligands was considerably shielded and electron-rich compared to Mor-Dalphos (${}^{31}\text{P}\{\text{H}\}$ δ = 20.4 ppm)²⁸ and PAd₃ (${}^{31}\text{P}\{\text{H}\}$ δ = 59.4 ppm).⁴⁸ The CH_2 (C_α from P) group in the 1-adamantyl moiety also showed a significant difference in the ${}^1\text{H}$ NMR spectra of all ligands, revealing the influence of nitrogen in proximity. The structures of **L2** and **L3** were further confirmed using single-crystal X-ray diffraction (scXRD),^{49–51} which showed a distorted pyramidal geometry on the P atom (Fig. 2B). All three ligands were stable in the solid state and

can be used on the benchtop. However, **L1** was sensitive to oxidation by air in the solution under ambient conditions (~9% oxidation after 48 h), whereas **L2** and **L3** were stable under the same conditions.

With the pure ligands, **L1–3**, in hand, we examined the complexation behavior with $\text{Pd}(\text{II})$. QAdPhos (**L1**) with PdCl_2 resulted in the expected $\kappa^2\text{-P}^\text{N}$ coordinated (**L1**) PdCl_2 (Fig. 2C). The observed downfield shift in ${}^{31}\text{P}\{\text{H}\}$ NMR at δ 82.6 ppm confirmed the P^N coordination. The Pd complex was structurally characterized using scXRD (Fig. 2E). The bite angle of $\angle\text{PPdN}$ was observed as 84.96° for (**L1**) PdCl_2 , which was close to that reported for the (4-(2-(di(1-adamantyl)phosphino)phenyl)morpholine) $\text{Pd}(\eta^1\text{-1-phenylallyl})$ chloride complex ($\angle\text{PPdN} = 85.27^\circ$).²⁹ The reaction of PdCl_2 with **L2** and **L3** resulted in an uncharacterizable insoluble white solid, possibly a polymeric mixture.

The reaction of $\text{Pd}(\text{OAc})_2$ with **L1** resulted in a P^N coordinated, $\mu\text{-OAc}$ bridged dimer with two OAc^- groups as counteranions $\{[(\text{L1})\text{Pd}(\text{OAc})_2]_2 2[\text{OAc}]^-\}$ (Fig. 2D). ATR-IR showed a broad band centered at 1603 cm^{-1} ($\nu_{\text{C=O}}$), and a sharp band at 1450 cm^{-1} ($\nu_{\text{C-O}}$), which were consistent with the reported values for acetate.^{52,53} The ${}^{31}\text{P}\{\text{H}\}$ NMR spectrum showed two peaks at 75.0 ppm (67%; *trans* isomer) and 74.4 ppm (33%; *cis* isomer). We speculate that the bulky Ad groups favor the *trans* isomer as the major isomer, as reported for the *t*Bu analog.^{19,34} The *cis*:*trans* isomer ratio was also observed in ${}^1\text{H}$ and ${}^{13}\text{C}\{\text{H}\}$ NMR spectra. The ESI-MS analysis showed the $[\text{C}_{31}\text{H}_{39}\text{PNO}_2\text{Pd}]^+$ fragment m/z value of 594 (100%), corresponding to a partial dimer fragment. The reaction of $\text{Pd}(\text{OAc})_2$ with **L2** resulted in a $\kappa^2\text{-P}^\text{C}$ -coordinated dimer, $[(\text{L2})\text{Pd}(\text{OAc})_2]$ (55%), *via* acetate bridging without an additional base, which suggested that the OAc^- group acted as a base and facilitated P^C coordination (Fig. 2D). For $[(\text{L2})\text{Pd}(\text{OAc})_2]$, ${}^{31}\text{P}\{\text{H}\}$ NMR showed a peak at 111.3 ppm, and the H8 proton peak ($\delta = 9.16\text{ ppm}$) of the ligand **L2** completely disappeared after Pd complexation, which confirmed the $\kappa^2\text{-P}^\text{C}$ coordination (Fig. S3 & S4; SI). ESI-MS analysis showed a $[\text{C}_{30}\text{H}_{36}\text{PPd}]^+$ fragment m/z value of 533 (100%), which matched the P^C -Pd coordinated fragment. Under similar reaction conditions, **L3** did not proceed towards $\kappa^2\text{-P}^\text{C}$ coordination as confirmed by ${}^{31}\text{P}\{\text{H}\}$ NMR. At higher temperature (130 °C) reaction of $\text{Pd}(\text{OAc})_2$ with **L3** resulted in the $\kappa^2\text{-P}^\text{C}$ coordinated complex $[(\text{L3})\text{Pd}(\text{OAc})_2]$. The dimer complex showed a peak at 105.7 ppm in ${}^{31}\text{P}\{\text{H}\}$ NMR, and the H1 proton peak ($\delta = 10.52\text{ ppm}$) of the ligand **L3** completely disappeared after Pd complexation (Fig. S5 & S6; SI). ESI-MS showed a $[\text{C}_{62}\text{H}_{76}\text{P}_2\text{N}_2\text{O}_4\text{Pd}_2]^+$ corresponding peak at an m/z value of 1188 (100%) for the dimer $[(\text{L3})\text{Pd}(\text{OAc})_2]$. The ATR-IR spectra showed that peaks corresponding to acetates were consistent with the reported values.^{52,53} All these characterization studies indicated the $\kappa^2\text{-P}^\text{N}/\text{P}^\text{C}$ coordinated Pd dimer complex for all ligands.

Understanding Pd complex formation further motivated us to investigate the catalytic performance of these ligands. To explore the catalytic performance of **L1–3**, we began our study by focusing on the Mizoroki–Heck reaction (Table 1; Tables



Table 1 Reaction method development^a

Entry	Conditions screened	3a (4a) ^b
1	L1; KOAc; 24 h	37 (5)
2	L2; KOAc; 24 h	19 (4)
3	L3; KOAc; 24 h	83 (7)
4	L3; KHCO ₃ ; 24 h	93 (7)
5	L3; KHCO ₃ ; 6 h	95 (5)
6 ^c	0.25 mol% [(L1)Pd(OAc) ₂] ₂ [OAc] ⁻	47 (6)
7 ^c	0.25 mol% [(L2)Pd(OAc) ₂] ₂	23 (2)
8 ^c	0.25 mol% [(L3)Pd(OAc) ₂] ₂	93 (7)
9	PhI instead of PhBr	93 (7)
10	PhX (X = Cl, OTf, OTs) instead of PhBr	Not observed

^a Optimized reaction conditions: bromobenzene (1 mmol), styrene (1.5 mmol), Pd(OAc)₂ (0.005 mmol), *i*QAdPhos/L3 (0.005 mmol), and KHCO₃ (1.5 mmol) in degassed DMA (0.25 M) under argon. ^b GC conversions. ^c Only a Pd complex was used as a catalyst. See Tables S1–S11 in the SI.

S1–S11 in SI). 0.5 mol% of Pd(OAc)₂/L3, in the presence of KOAc in 0.25 M DMA, showed 83% 3a and 7% 4a after 24 h at 130 °C. Temperatures lower than 130 °C resulted in traces of 3a (Table S4; SI). Among the Pd sources screened, Pd(OAc)₂ was found to be the most efficient (Table S5; SI). KOAc resulted in 83% 3a; however, the milder base KHCO₃, a better alternative for hygroscopic KOAc, showed 93% 3a. Other bases

resulted in 2–80% conversion (Table S6, SI). Commercially available phosphine ligands like PPh₃ and 1,3-bis(diphenylphosphino)propane (dppp) showed 19–26% of 3a under these conditions (Table S7, SI). Further decreasing the reaction time to 6 h gave 95% 3a (TOF = 31.6 h⁻¹) and 5% 4a (Table 1), as supported by the reaction profile obtained from gas chromatography (Fig. S7 and S8, SI). When the synthesized [(L1)Pd(OAc)₂]₂[OAc]⁻, [(L2)Pd(OAc)₂]₂, and [(L3)Pd(OAc)₂]₂ complexes were used as catalysts, they yielded 47%, 23% and 93% of 3a, respectively, indicating that the ligand-coordinated Pd complex might be an active catalyst or pre-catalyst (Table 1). Reaction using 0.5 mol% Pd(OAc)₂ with 2, 3, and 5 equivalents of L3 resulted in 21%, 8%, and <1% of 3a, respectively, suggesting that bis-coordination deactivates the catalyst. Furthermore, it indicated that the Pd(II) to Pd(0) reduction might have occurred due to high temperature and the presence of KHCO₃ (Table S11, SI), not by phosphine ligand oxidation.^{54,55} The reaction conditions were also compatible with aryl iodides, yielding conversions comparable to those of aryl bromides (Table 1). Aryl chloride and aryl pseudohalides failed to react under the optimized conditions (Table 1). The control reactions revealed that all reactants and catalysts were necessary to obtain product 3a. Without L3, only 12% 3a was observed, supporting the ligand-controlled catalytic cycle (SI).

The optimized conditions were further explored for various substrates bearing electronic and steric factors (Fig. 3). Bromobenzene resulted in 89% (TOF = 29.6 h⁻¹; 6 h) isolated yield of *E*-stilbene (3a) and 85% isolated yield for a large-scale reaction (5 mmol, 0.785 g) using 0.1 mol% catalyst loading (TOF = 141.9 h⁻¹; 30 h). Electron-donating substituents, such

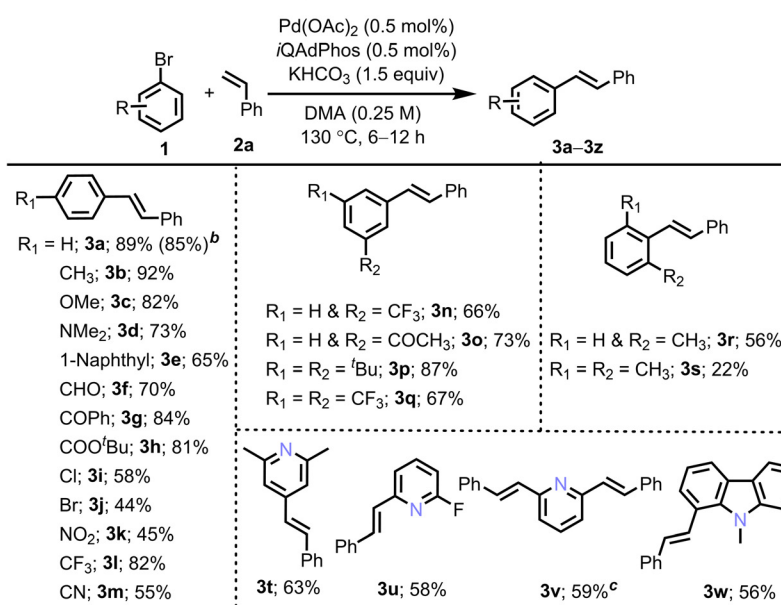
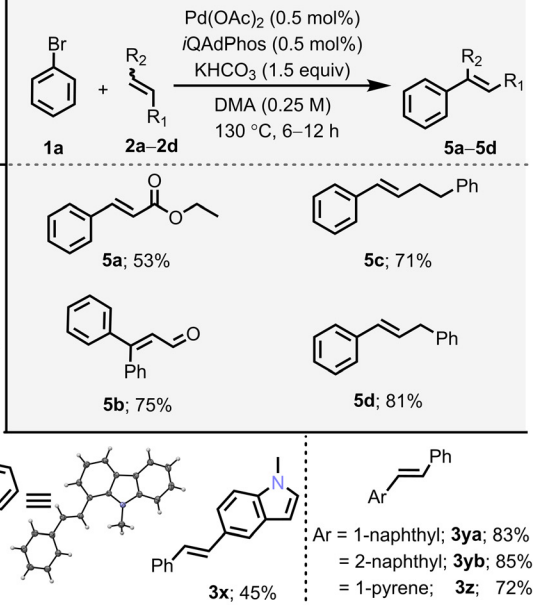
A) Aryl bromide substrate scope^aB) Alkene substrate scope^a

Fig. 3 Substrate scope. ^a Reaction conditions: aryl bromide (1 mmol), alkene (1.5 mmol), Pd(OAc)₂ (0.005 mmol), *i*QAdPhos (0.005 mmol), and KHCO₃ (1.5 mmol) in degassed DMA (0.25 M) for 6–12 h at 130 °C under argon. The reported isolated yields are the average of at least two reactions. ^b 5 mmol PhBr reaction scale using a 0.1 mol% catalyst loading for 30 h and ^c 5 equivalents of styrene and KHCO₃ were used.

as *p*-Me (**3b**), *p*-OMe (**3c**), *p*-NMe₂(**3d**), and *p*-1-naphthyl (**3e**), resulted in 65–92% yields. They were also suitable for various reactive functional groups, such as *p*-CHO (**3f**; 70%), *p*-COPh (**3g**; 84%), and *p*-COO'Bu (**3h**; 81%). The halogen substituents, *p*-Cl and *p*-Br, resulted in 58% (**3i**) and 44% (**3j**) yields, respectively, with the retention of one Cl and Br. EWGs, such as *p*-NO₂ (**3k**), *p*-CF₃ (**3l**), and *p*-CN (**3m**), yielded the desired products (45–82%). *m* and *m,m'* substituted derivatives such as **3n** (66%), **3o** (73%), **3p** (87%), and **3q** (67%) were obtained in good yields. *o*-Me (**3r**; 56%) and *o,o'*-Me (**3s**; 22%) furnished moderate yields, probably due to steric reasons. The pyridine heterocycles also worked well under these conditions, resulting in **3t** (63%), **3u** (58%), and **3v** (59%). 1-Bromo-9-methyl-9*H*-carbazole and 5-bromo-1-methyl-1*H*-indole yielded 56% (**3w**; structurally characterized) and 45% (**3x**) of the desired product, respectively. 1-Bromonaphthalene, 2-bromonaphthalene, and 1-bromopyrene substrates gave good yields of **3y** (83%), **3yb** (85%), and **3z** (72%), respectively. The α,β -unsaturated carbonyl derivatives were tolerated under the optimized reaction conditions and yielded the desired *E* product in 53% (**5a**) and 75% (**5b**) yields. Allylbenzene and 4-phenyl-1-butene also gave 71% (**5c**) and 81% (**5d**) yields of the major products with a minor geminal isomer as observed in ¹H NMR spectra (<10%; SI). We found that a few substrates (unactivated olefins, reactive heterocycles, etc.) showed either complex or no reactivity (SI).

In conclusion, we synthesized a series of bulky di(1-adamantyl)(aryl)phosphine {P(1-Ad)₂(Ar)} ligands, **L1–3**, featuring quinoline, naphthyl, and isoquinoline substituents, enabling the formation of Pd(II) complexes that coordinate through κ^2 -P^N and P^C modes. Among these, the ligand *i*QAdPhos (**L3**) showed excellent catalytic activity with 0.5 mol% Pd(OAc)₂ (TOF = 29.6 h⁻¹). The catalyst loading could be further reduced to 0.1 mol% by extending the time (TOF = 141.9 h⁻¹). We tested a variety of (hetero)aryl bromides and alkenes, achieving moderate to excellent yields of the Mizoroki–Heck coupling products (22–92% isolated yields). This study demonstrates the potential of bulky P(1-Ad)₂(Ar) ligands in Pd-catalyzed C–C bond formation and offers valuable insights into ligand design and Pd coordination.

Conflicts of interest

There are no conflicts to declare.

Data availability

Supplementary information (SI): experimental and spectral data. See DOI: <https://doi.org/10.1039/d5dt02523k>.

CCDC 2469531 (**L2**), 2469533 (**L3**), 2469538 (**L1**) PdCl₂·3CH₂Cl₂) and 2495634 (**3w**) contain the supplementary crystallographic data for this paper.^{56a–d}

Acknowledgements

All authors thank the Indian Institute of Technology Goa (IIT Goa) for the infrastructure and Max-Planck-Gesellschaft (MPG) and Max-Planck-Institut für Kohlenforschung (MPI Kofo) for the generous funding through the “Max Planck India partner group” project. We are grateful to Prof. Benjamin List for his support throughout this project. We thank Ms. Nikita G. and Prof. Sunder N. Dhuri, Goa University, and Mr. Sivaraj Chandrasekaran, VIT, Chennai, for the scXRD data.

References

- 1 D. S. Surry and S. L. Buchwald, *Chem. Sci.*, 2010, **2**, 27–50.
- 2 L.-C. Campeau and N. Hazari, *Organometallics*, 2019, **38**, 3–35.
- 3 P. G. Gildner and T. J. Colacot, *Organometallics*, 2015, **34**, 5497–5508.
- 4 T. L. Brown and K. J. Lee, *Coord. Chem. Rev.*, 1993, **128**, 89–116.
- 5 M. Kranenburg, P. C. J. Kamer, P. W. N. M. van Leeuwen, D. Vogt and W. Keim, *J. Chem. Soc., Chem. Commun.*, 1995, 2177–2178.
- 6 C. A. Tolman, *Chem. Rev.*, 1977, **77**, 313–348.
- 7 Z. Freixa and P. W. N. M. van Leeuwen, *Dalton Trans.*, 2003, 1890–1901.
- 8 J. F. Hartwig, *Inorg. Chem.*, 2007, **46**, 1936–1947.
- 9 D. S. Surry and S. L. Buchwald, *Angew. Chem., Int. Ed.*, 2008, **47**, 6338–6361.
- 10 H.-J. Xu, Y.-Q. Zhao and X.-F. Zhou, *J. Org. Chem.*, 2011, **76**, 8036–8041.
- 11 C. Sivarajan, S. Saha, S. Mulla and R. Mitra, *J. Org. Chem.*, 2024, **89**, 17021–17030.
- 12 P. Schiltz, N. Casaretto, S. Bourcier, A. Auffrant and C. Gosmini, *Dalton Trans.*, 2023, **52**, 14859–14866.
- 13 J. James, M. Jackson and P. J. Guiry, *Adv. Synth. Catal.*, 2019, **361**, 3016–3049.
- 14 P. J. Guiry and C. P. Saunders, *Adv. Synth. Catal.*, 2004, **346**, 497–537.
- 15 H. A. Hudali, J. V. Kingston and H. A. Tayim, *Inorg. Chem.*, 1979, **18**, 1391–1394.
- 16 G. Sabharwal, K. C. Dwivedi and M. S. Balakrishna, *Dalton Trans.*, 2025, **54**, 11551–11562.
- 17 J. Monot, E. Marelli, B. Martin-Vaca and D. Bourissou, *Chem. Soc. Rev.*, 2023, **52**, 3543–3566.
- 18 J. Dupont, C. S. Consorti and J. Spencer, *Chem. Rev.*, 2005, **105**, 2527–2572.
- 19 W. A. Herrmann, C. Brossmer, C.-P. Reisinger, T. H. Riermeier, K. Öfele and M. Beller, *Chem. – Eur. J.*, 1997, **3**, 1357–1364.
- 20 F. Schroeter, J. Soellner and T. Strassner, *ACS Catal.*, 2017, **7**, 3004–3009.
- 21 L. Canovese, C. Santo and F. Visentin, *Organometallics*, 2008, **27**, 3577–3581.
- 22 T. Tsukuda, C. Nishigata, K. Arai and T. Tsubomura, *Polyhedron*, 2009, **28**, 7–12.
- 23 T. Suzuki, *Bull. Chem. Soc. Jpn.*, 2004, **77**, 1869–1876.



24 Y. Canac, *Chem. Rec.*, 2023, **23**, e202300187.

25 J. James and P. J. Guiry, *ACS Catal.*, 2017, **7**, 1397–1402.

26 S. Jin, L. Liu and F. Lin, *Organometallics*, 2025, **44**, 2025–2034.

27 R. J. Lundgren, K. D. Hesp and M. Stradiotto, *Synlett*, 2011, 2443–2458.

28 R. J. Lundgren, B. D. Peters, P. G. Alsabeh and M. Stradiotto, *Angew. Chem., Int. Ed.*, 2010, **49**, 4071–4074.

29 P. G. Alsabeh, R. J. Lundgren, R. McDonald, C. C. C. Johansson Seechurn, T. J. Colacot and M. Stradiotto, *Chem. – Eur. J.*, 2013, **19**, 2131–2141.

30 K. M. Morrison and M. Stradiotto, *Chem. Sci.*, 2024, **15**, 7394–7407.

31 A. B. Gade, Urvashi and N. T. Patil, *Org. Chem. Front.*, 2024, **11**, 1858–1895.

32 P. Schiltz, N. Casaretto, A. Auffrant and C. Gosmini, *Chem. – Eur. J.*, 2022, **28**, e202200437.

33 S. Kelly, R. Goddard and P. J. Guiry, *Helv. Chim. Acta*, 2022, **105**, e202100205.

34 L. Canovese, F. Visentin, G. Chessa, C. Santo and A. Dolmella, *Dalton Trans.*, 2009, 9475–9485.

35 L. Canovese, F. Visentin, T. Scattolin, C. Santo and V. Bertolasi, *Dalton Trans.*, 2015, **44**, 15049–15058.

36 T. Scattolin, F. Visentin, C. Santo, V. Bertolasi and L. Canovese, *Dalton Trans.*, 2017, **46**, 5210–5217.

37 T. Suzuki, H. Yamaguchi, M. Fujiki, A. Hashimoto and H. D. Takagi, *Acta Crystallogr., Sect. E: Crystallogr. Commun.*, 2015, **71**, 447–451.

38 G. D. Frey, C.-P. Reisinger, E. Herdtweck and W. A. Herrmann, *J. Organomet. Chem.*, 2005, **690**, 3193–3201.

39 C. Amatore and A. Jutand, *Acc. Chem. Res.*, 2000, **33**, 314–321.

40 B. L. Shaw, *Chem. Commun.*, 1998, 1361–1362.

41 M. Beller, H. Fischer, W. A. Herrmann, K. Öfele and C. Grossmer, *Angew. Chem., Int. Ed. Engl.*, 1995, **34**, 1848–1849.

42 W. A. Herrmann, C. Grossmer, K. Öfele, C.-P. Reisinger, T. Priermeier, M. Beller and H. Fischer, *Angew. Chem., Int. Ed. Engl.*, 1995, **34**, 1844–1848.

43 T. Mizoroki, K. Mori and A. Ozaki, *Bull. Chem. Soc. Jpn.*, 1971, **44**, 581.

44 R. F. Heck and J. P. Nolley Jr., *J. Org. Chem.*, 1972, **37**, 2320–2322.

45 N. Tashima, T. Sawazaki, Y. Kayaki and S. Kuwata, *Chem. Lett.*, 2019, **48**, 787–790.

46 J. R. Goerlich and R. Schmutzler, *Phosphorus, Sulfur Silicon Relat. Elem.*, 1995, **102**, 211–215.

47 Á. Sinai, D. C. Simkó, F. Szabó, A. Paczal, T. Gáti, A. Bényei, Z. Novák and A. Kotschy, *Eur. J. Org. Chem.*, 2020, 1122–1128.

48 L. Chen, P. Ren and B. P. Carrow, *J. Am. Chem. Soc.*, 2016, **138**, 6392–6395.

49 O. V. Dolomanov, L. J. Bourhis, R. J. Gildea, J. A. K. Howard and H. Puschmann, *J. Appl. Crystallogr.*, 2009, **42**, 339–341.

50 G. M. Sheldrick, *Acta Crystallogr., Sect. A: Found. Adv.*, 2008, **64**, 112–122.

51 G. M. Sheldrick, *Acta Crystallogr., Sect. A: Found. Crystallogr.*, 2015, **71**, 3–8.

52 E. Spinner, *J. Chem. Soc.*, 1964, 4217–4226.

53 F. Villalba, S. Martín-Martín and A. C. Albéniz, *ChemCatChem*, 2025, e00335.

54 T. Fantoni, C. Palladino, R. Grigolato, B. Muzzi, L. Ferrazzano, A. Tolomelli and W. Cabri, *Org. Chem. Front.*, 2025, **12**, 1982–1991.

55 F. d'Orlyé and A. Jutand, *Tetrahedron*, 2005, **61**, 9670–9678.

56 (a) CCDC 2469531: Experimental Crystal Structure Determination, 2025, DOI: [10.5517/ccdc.csd.cc2nwr9m](https://doi.org/10.5517/ccdc.csd.cc2nwr9m);
 (b) CCDC 2469533: Experimental Crystal Structure Determination, 2025, DOI: [10.5517/ccdc.csd.cc2nwrcp](https://doi.org/10.5517/ccdc.csd.cc2nwrcp);
 (c) CCDC 2469538: Experimental Crystal Structure Determination, 2025, DOI: [10.5517/ccdc.csd.cc2nwrjv](https://doi.org/10.5517/ccdc.csd.cc2nwrjv);
 (d) CCDC 2495634: Experimental Crystal Structure Determination, 2025, DOI: [10.5517/ccdc.csd.cc2prxbq](https://doi.org/10.5517/ccdc.csd.cc2prxbq).

